

Cell Reports, Volume 37

Supplemental information

**Contribution of autophagy machinery factors to
HCV and SARS-CoV-2 replication organelle formation**

Woan-Ing Twu, Ji-Young Lee, Heeyoung Kim, Vibhu Prasad, Berati Cerikan, Uta Haselmann, Keisuke Tabata, and Ralf Bartenschlager

1 **Supplemental Information**

2

3

4 **Contribution of autophagy machinery factors to HCV and SARS-CoV-2**
5 **replication organelle formation**

6

7 Woan-Ing Twu, Ji-Young Lee, Heeyoung Kim, Vibhu Prasad, Berati Cerikan, Uta

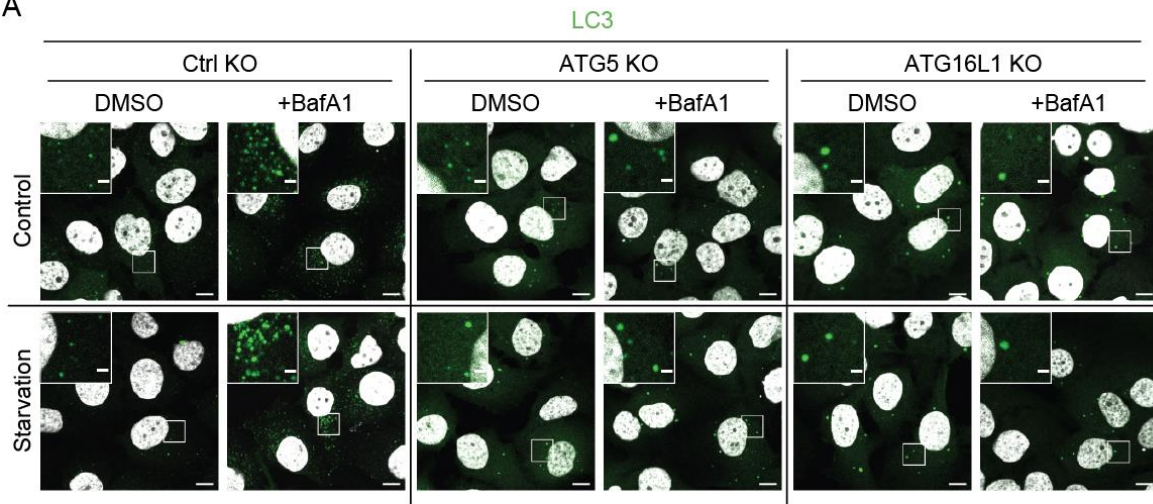
8 Haselmann, Keisuke Tabata and Ralf Bartenschlager

9

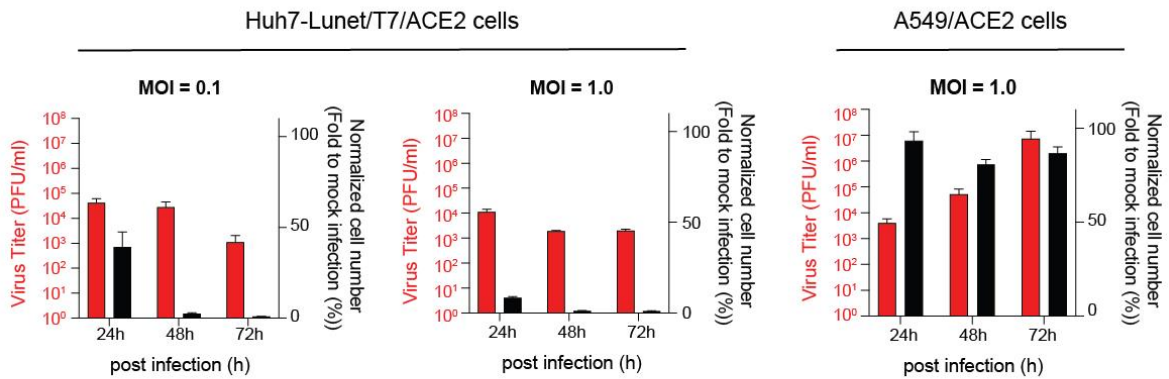
10

11 **Figure S1**

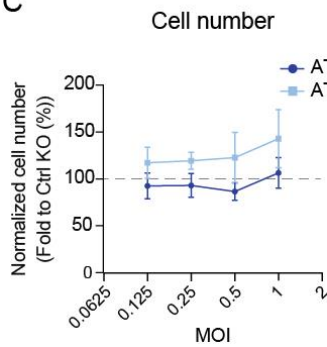
A



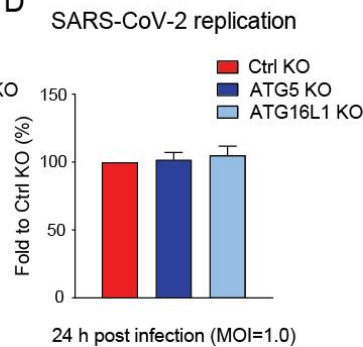
B



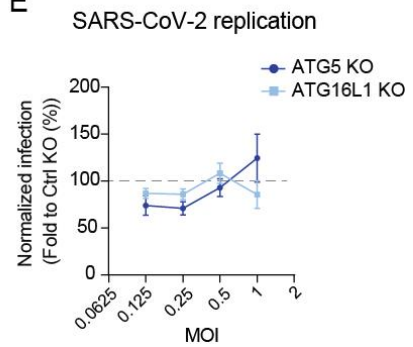
C



D



E



12

13

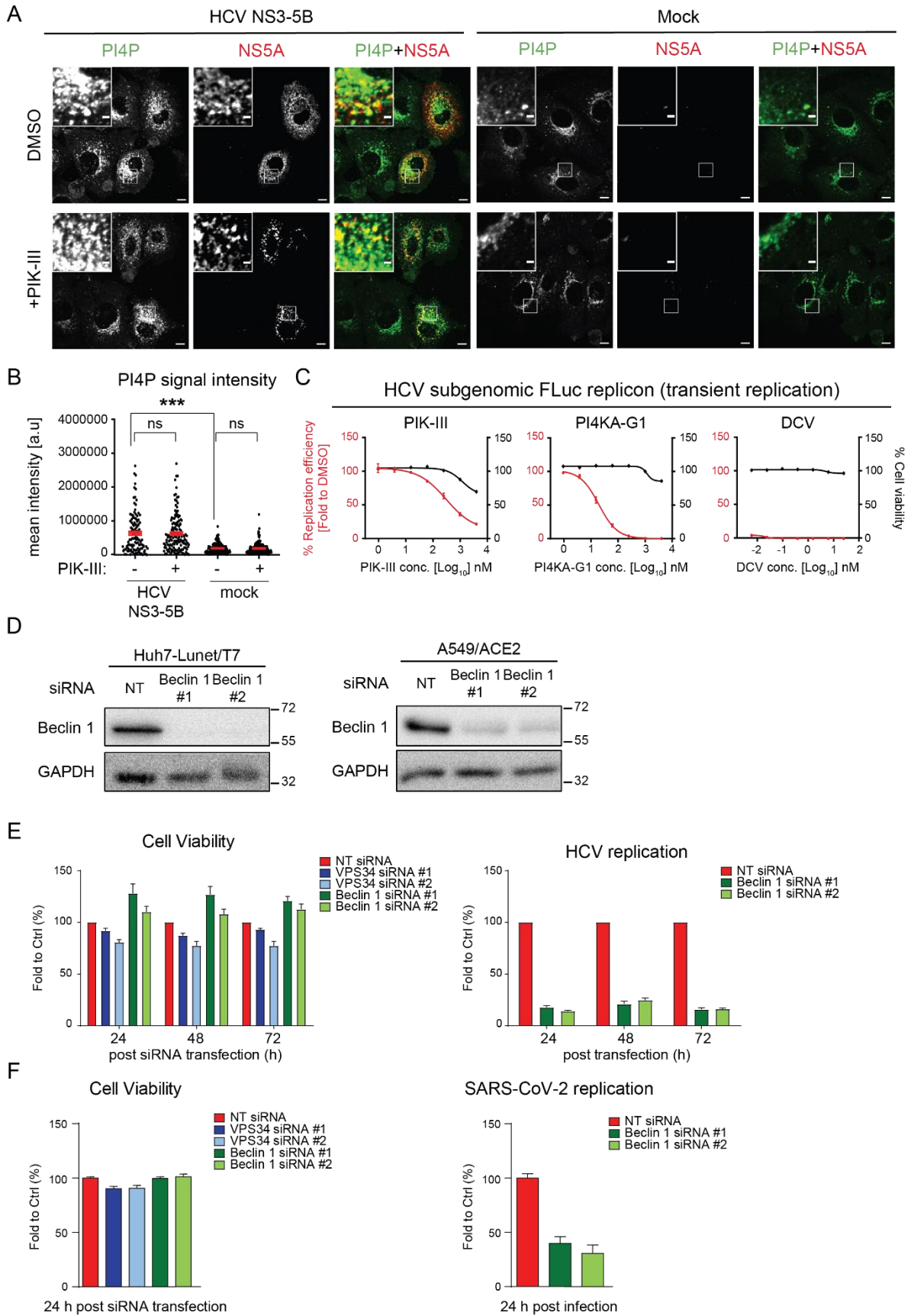
14 **Figure S1. Functional validation of AGT5 and ATG16L1 KO and replication of**
 15 **SARS-CoV-2 in different cell lines including KO cell pools.** Related to Figure 1.

16 (A) Huh7-Lunet/T7 cells with ATG5 or ATG16L1 KO were subjected to starvation or
 17 cultured under regular conditions and treated or not with 100 nM Bafilomycin A1
 18 (BafA1) for 2 h prior to fixation. Fixed cells were stained for LC3. Upper-left inserts
 19 show magnifications of white boxed areas in each image. Scale bar for overview

20 image, 10 μm ; for magnified image, 2 μm . Quantification of a larger set of images is
21 given in Figure 1E. (B) Replication kinetics of SARS-CoV-2 in Huh7-Lunet/T7/ACE2
22 and A549/ACE2 cells after infection at different MOIs. Titers of infectious virus were
23 determined by plaque assay and cell numbers were analyzed by DAPI staining
24 followed by CellProfiler image analysis. Data represent mean \pm SEM from two
25 independent experiments. (C-E) Huh7-Lunet/T7/ACE2 cells with given ATG KO or
26 control KO cells were infected with SARS-CoV-2 at indicated MOI. (C) Total cell
27 numbers (minimum 5,000 cells per sample) were analyzed by DAPI staining
28 followed by CellProfiler image analysis at 24 h post-infection. Values were
29 normalized to those of infected control KO cells (set to 100% as indicated with the
30 dotted horizontal line). Data represent mean \pm SEM from two independent
31 experiments. (D) Cells were infected as in panel (C) at MOI = 1. After 24 h, virus
32 replication was determined by measuring the amount of SARS-CoV-2 nucleocapsid
33 protein using immunostaining. Data represent mean \pm SEM from three independent
34 experiments. (E) Cells were infected with SARS-CoV-2 at MOIs specified on the
35 bottom and fixed 16 h later. Virus replication was determined using nucleocapsid
36 protein (N) staining and the percentage of N-positive cells was determined using the
37 CellProfiler image analysis software package. Percentage infection for ATG5 or
38 ATG16L1 KO cells was calculated by normalization of values to those obtained with
39 control KO cells. Normalized data from 3 biologically independent experiments are
40 plotted. Data represent mean \pm SEM from two independent experiments.

41

42 **Figure S2**



43

44

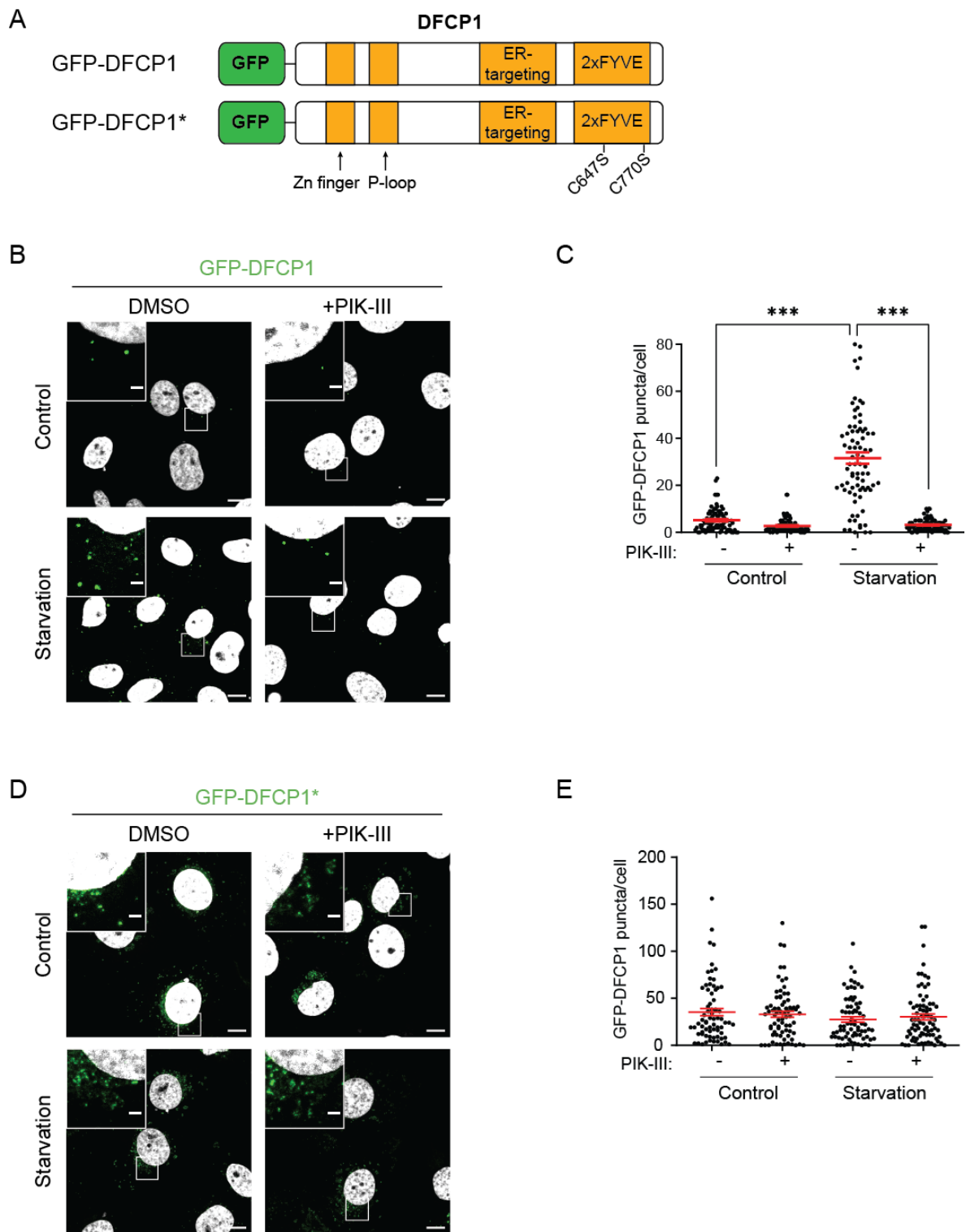
45 **Figure S2. Evaluation of knockdown of the PI3K core components VPS34 and**
46 **Beclin1 and impairment of HCV and SARS-CoV-2 replication upon Beclin1**
47 **depletion.** Related to Figure 2.

48 (A-B) Pharmacological inhibition of PI3K does not affect PI4P levels. Huh7-Lunet/T7
49 cells were transfected with the HCV NS3-5B expression construct and on the next
50 day treated with DMSO or 1 μ M PIK-III for 2 h. Fixed cells were stained with PI4P-
51 and NS5A-specific antibodies. (A) Upper-left inserts show magnifications of white
52 boxed areas in each image. Scale bar for overview image, 10 μ m; for magnified
53 image, 2 μ m. (B) Quantification of PI4P puncta. At least 80 cells were analyzed in
54 each sample by using the “Analyzed Particles” function in ImageJ. Data represent
55 mean \pm SEM from two independent experiments. *** p <0.001; ns, non-significant. (C)
56 Huh7-Lunet/T7 cells were transfected with a subgenomic HCV reporter replicon.
57 After 4 h, cells were treated with different concentrations of drugs given on the top of
58 each panel. Luciferase activity reflecting HCV replication efficiency and cell viability
59 were measured at 24 h post-transfection. DCV, Daclatasvir. (D) Beclin 1 depletion by
60 KD in Huh7-Lunet/T7 and A549/ACE2 cells was determined by western blotting.
61 GAPDH served as loading control. (E) Left panel: Effect of VPS34 (corresponding to
62 Figure 2C) and Beclin 1 KD on viability of Huh7-Lunet/T7 cells as determined by
63 Celltiter Glo assay (measuring ATP content) 24, 48, and 72 h after the last siRNA
64 transfection. Right panel: Luciferase activity reflecting HCV RNA replication was
65 measured 24, 48, and 72 h post HCV replicon RNA transfection. (F) Left panel:
66 Effect of VPS34 (corresponding to Figure 2G) and Beclin 1 KD on viability of
67 A549/ACE2 cells (measuring ATP content) was determined 24 h after the last siRNA
68 transfection. Right panel: Percentage of SARS-CoV-2 replication was determined by
69 N-protein specific immune-staining 24 h post-infection. Data in (C), (E), and (F)
70 represent the mean \pm SEM from three independent experiments.

71

72 **Figure S3**

73



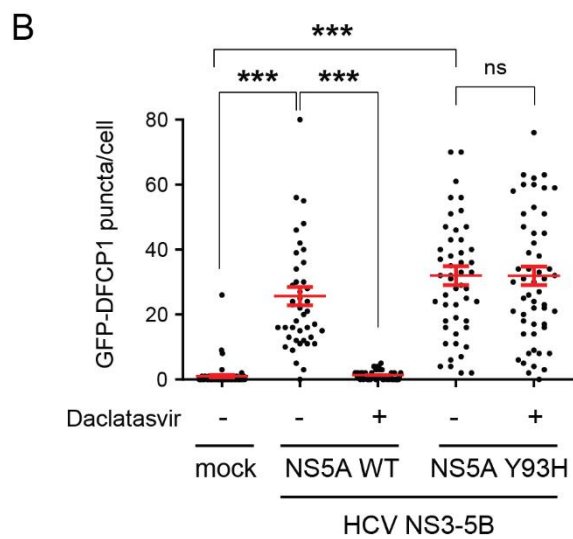
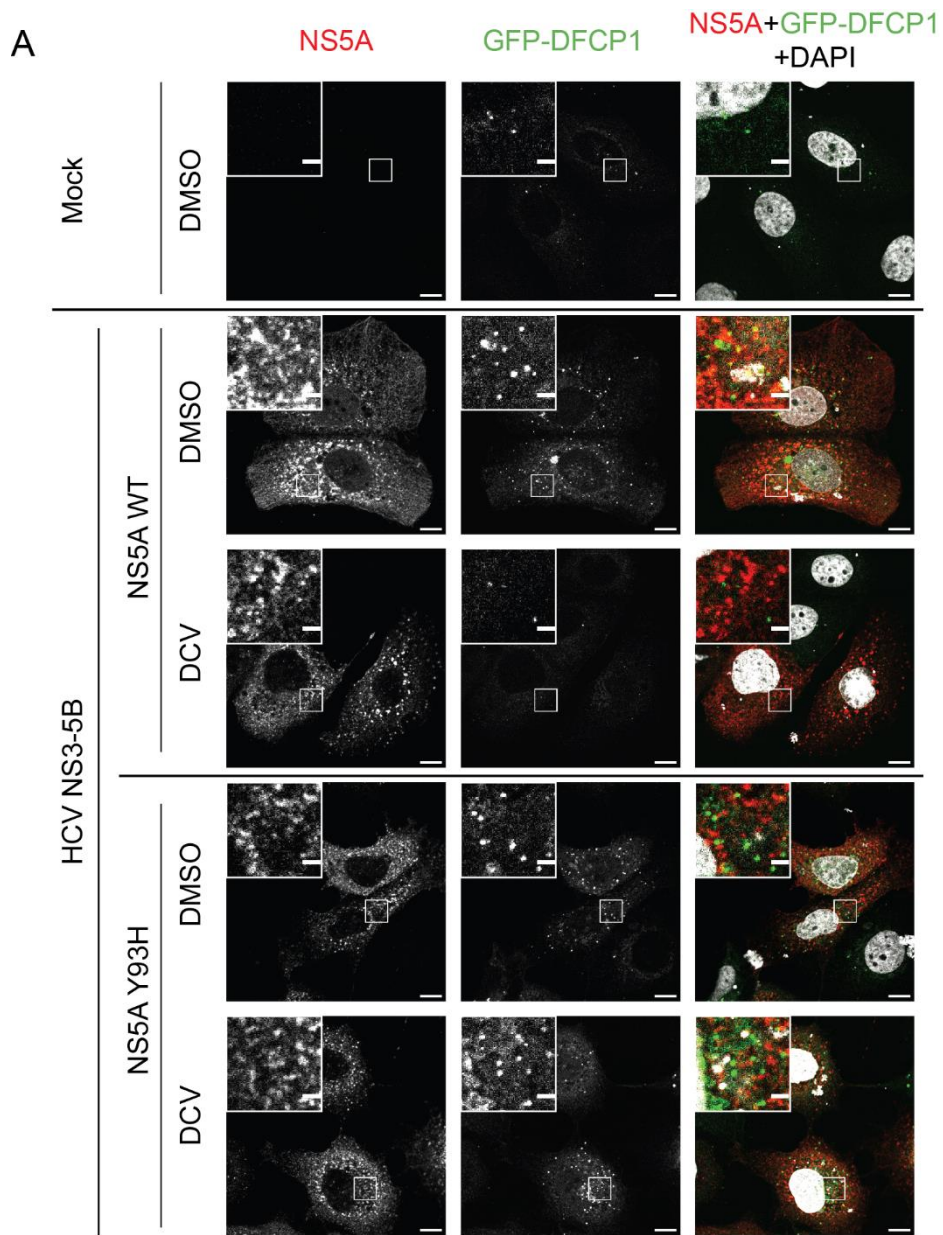
74

75

76

77

78 **Figure S3. Generation and validation of the intracellular PI3P sensor**
79 **GFP-DFCP1.** Related to Figure 3.
80 (A) Schematic depiction of the GFP-DFCP1 and GFP-DFCP1* (mutant) probes. The
81 latter contains the two given amino acid substitutions disrupting PI3P binding (Axe et
82 al., 2008). (B, C) Huh7-Lunet/T7 cell pools stably expressing GFP-DFCP1 were
83 subjected to starvation or cultured under normal conditions (control) and treated or
84 not with 1 μ M PIK-III for 2 h. (B) Representative confocal microscopy images
85 showing the subcellular distribution of GFP-DFCP1. Upper-left inserts show
86 magnifications of white boxed areas. (C) Quantification of GFP-DFCP1 puncta. At
87 least 80 cells were analyzed for each condition. (D, E) Huh7-Lunet/T7 cells stably
88 expressing the sensor mutant GFP-DFCP1* were treated and analyzed as
89 described for (B) and (C). Scale bar for overview image, 10 μ m; for magnified image,
90 2 μ m. All data represent mean \pm SEM from three independent experiments.
91 *** $p < 0.001$.
92



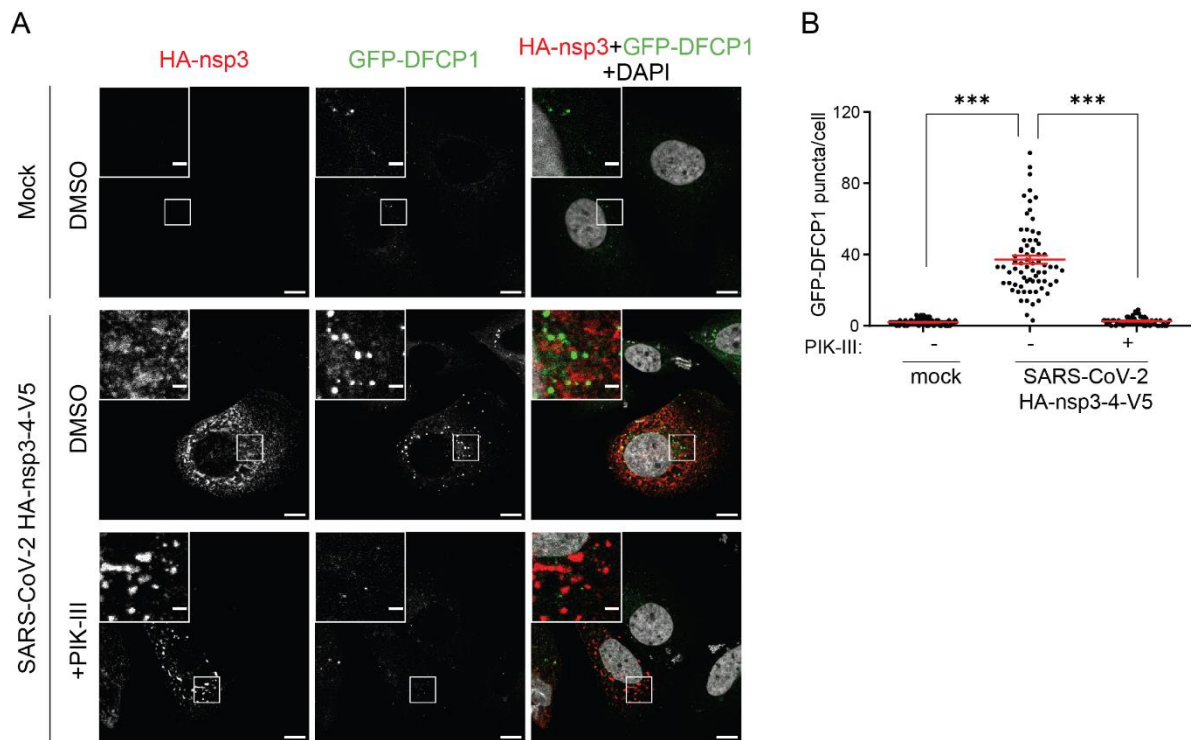
94 **Figure S4. NS5A is required for HCV NS3-5B induced increase of PI3P.** Related
95 to Figure 3.

96 Huh7-Lunet/T7 cells stably expressing GFP-DFCP1 were transfected with the HCV
97 NS3-5B expression plasmid encoding either NS5A wildtype (WT) or NS5A Y93H, a
98 mutation conferring high-level resistance to the NS5A inhibitor Daclatasvir (DCV).
99 After 5 h, cells were treated with 1 nM DCV and cells were fixed 24 h after
100 transfection. (A) Representative confocal microscopy images showing the
101 subcellular distribution of GFP-DFCP1 and NS5A. Upper-left inserts show
102 magnifications of white boxed areas. (B) Quantification of GFP-DFCP1 puncta. At
103 least 50 cells were analyzed for each condition. Scale bar for overview image, 10
104 μm ; for magnified image, 2 μm . Data represent mean \pm SEM from two independent
105 experiments. *** $p < 0.001$; ns, no significant.

106

107 **Figure S5**

108



109

110

111 **Figure S5. SARS-CoV-2 nsp3-4 expression increases intracellular PI3P levels.**

112 Related to Figure 3.

113 Huh7-Lunet/T7 cells stably expressing GFP-DFCP1 were transfected with the
114 SARS-CoV-2 HA-nsp3-4-V5 expression construct to induce the formation of DMVs.

115 After 24 h, cells were treated with 1 μ M PIK-III for 2 h prior to fixation. (A)

116 Representative confocal microscopy images showing the subcellular distribution of
117 GFP-DFCP1 and SARS-CoV-2 HA-nsp3. Upper-left inserts show magnifications of

118 white boxed areas. (B) Quantification of GFP-DFCP1 puncta. At least 60 cells were
119 analyzed for each condition. Scale bars for overview images, 10 μ m; for magnified

120 images, 2 μ m. Data represent mean \pm SEM from two independent experiments.

121 *** $p < 0.001$.

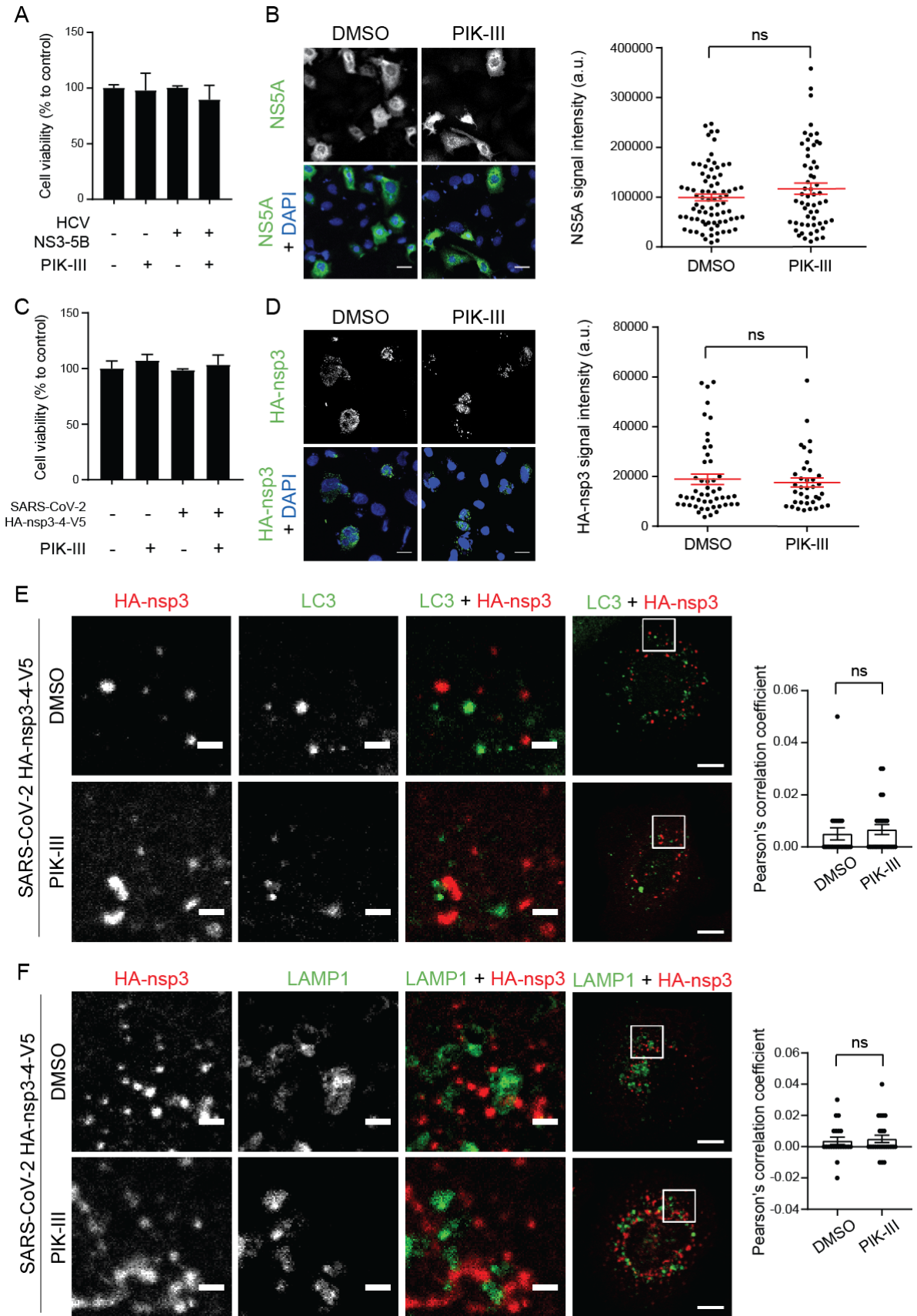
122

123

124

125

126



130 **Figure S6. No evidence for enhanced degradation of HCV NS3-5B and**
131 **SARS-CoV-2 nsp3-4 upon pharmacological inhibition of PI3K.** Related to Figure
132 4.

133 (A-B) Huh7-Lunet/T7 cells were transfected with the HCV NS3-5B expression
134 plasmid. After 5 h, 1 μ M PIK-III was added to the cells that were lysed or fixed 24 h
135 after transfection to measure cell viability or NS5A, respectively. (A) Cell viability was
136 determined using WST-1 assay. Data represent mean \pm SEM from two independent
137 experiments. (B) Fixed cells were stained for NS5A and nuclear DNA was stained
138 with DAPI. NS5A signal intensity from 5 randomly selected areas was quantified by
139 using ImageJ. Scale bar, 30 μ m. (C-F) Huh7-Lunet/T7 cells were transfected with
140 the SARS-CoV-2 HA-nsp3-4-V5 expression plasmid and 24 h later, 1 μ M PIK-III was
141 added to the cells. After 48 h, cells were lysed or fixed for further analysis. (C) Cell
142 viability was determined by using WST-1 assay. (D) Fixed cells were stained for
143 HA-nsp3 by using a HA-specific antibody and signal intensity from 5 randomly
144 selected areas was quantified using ImageJ. Scale bar, 30 μ m. Data in (A-D)
145 represent mean \pm SEM. In (B) and (D), ns, not significant, according to two tailed,
146 unpaired Student's t-test. (E, F) Fixed cells were stained for (E) HA-nsp3 and LC3, or
147 (F) HA-nsp3 and LAMP1. The boxed area in the overview panel in the right indicates
148 the magnified region that is displayed in the other panels. Scale bars in the overview
149 and enlarged section represent 10 μ m and 2 μ m, respectively. The degrees of
150 colocalization between HA-nsp3 and LC3, or LAMP1 and LC3, were quantified by
151 determining Pearson's correlation coefficients. Analyses are based on at least 20
152 cells per condition. Data in (E) and (F) represent mean \pm SEM from two independent
153 experiments. ns, not significant, according to two tailed, unpaired Student's t-test.
154

155 **Table S1. Oligonucleotides.** Related to STAR METHODS.

156

Oligonucleotide name: Sequence	Source	Identifier
siRNA: NT Control	Life Technologies	4390846
siRNA: VPS34 #1: GCUUAGACCUGUCGGAUGATT	Life Technologies	s10519
siRNA: VPS34 #2: GCAUGGAGAUGAUUUACGUTT	Life Technologies	s10518
siRNA: Beclin 1 #1: CAGUUACAGAUGGAGCUUAATT	Life Technologies	s16537
siRNA: Beclin 1 #2: CAGAUACUCUUUUAGACCATT	Life Technologies	s16539
siRNA: DFCP1 #1: GGAUGGGUCUCGCAAAAUATT	Life Technologies	s28712
siRNA: DFCP1 #2: GGAUGUAAGAAAAGCAUGATT	Life Technologies	s28713
PCR primer: GFP-DFCP1_BamHI_F: AAAAGGATCCGCCACCATGGTGAGCAA GGGCGAG	Merck, Darmstadt, Germany	N/A
PCR primer: GFP-DFCP1_NotI_R: AAAAGCGGCCGCTTAAAGGTCACCGGG CTTTTTATTG	Merck, Darmstadt, Germany	N/A
PCR primer: DFCP1_FYVE*1_F: AGTCGGTGTCCGAGCTTAGCCTTGAC CCACCAAGG	Merck, Darmstadt, Germany	N/A
PCR primer: DFCP1_FYVE*1_R: CCTGGCTTCGTAGCTGTTGTCACAGAC	Merck, Darmstadt, Germany	N/A
PCR primer: DFCP1_FYVE*2_F: TGACAACAGCTACGAAGCCAGGAACG	Merck, Darmstadt, Germany	N/A
PCR primer: DFCP1_FYVE*2_R: TGCGGCCGCTTAAAGGTCACCGGGCTT TTTATTGCTGTTG	Merck, Darmstadt, Germany	N/A
PCR primer: piRO_SARS2_F: CACCTGATAATCTAGATAAGCACCAATC TTAGTGTTG	Merck, Darmstadt, Germany	N/A
PCR primer: piRO_SARS2_R: TGGCACGCGTGAATTCGGGCCCGGGAT TTTCCT	Merck, Darmstadt, Germany	N/A

157